ELSEVIER

Polymer 41 (2000) 4767–4780

polymer

Optically active polymethacrylates with side-chain L-lactic acid residues connected to push–pull azobenzene chromophores

L. Angiolini[a], D. Caretti[a], L. Giorgini[a], E. Salatelli[a], A. Altomare[b], C. Carlini[b,*], R. Solaro[b]

[a]*Dipartimento di Chimica Industriale e dei Materiali, University of Bologna, Viale Risorgimento 4, 40136 Bologna, Italy*
[b]*Dipartimento di Chimica e Chimica Industriale, University of Pisa, Via Risorgimento 35, 56126 Pisa, Italy*

Received 23 July 1999; received in revised form 20 September 1999; accepted 28 September 1999

Abstract

Novel optically active methacrylic homopolymers with side-chain L-lactic acid moieties interposed through ester bonds between the main chain and *trans*-4-azobenzene chromophores bearing in the 4′-position electron withdrawing groups, such as the cyano and nitro residues, have been synthesized and structurally characterized. Investigation by circular dichroism of the chiroptical and conformational properties of the polymers in solution indicates a much higher optical activity of these latter with respect to that of the corresponding low molecular weight model compounds, purposely prepared, due to the presence of dissymmetric conformations of one prevailing handedness. The *trans* to *cis* photoisomerization kinetics of the azoaromatic double bond has been measured in solution for polymers and models and the resulting data compared with those of previously reported similar photochromic derivatives. The influence of the nature of the electron withdrawing group in the 4′-position of the azobenzene chromophore on the chiroptical properties of the polymers is also discussed.

Keywords: Photochromic optically active polymers; Azobenzene-containing methacrylic polymers; Photoresponsive properties

1. Introduction

We have recently proposed the synthesis of a novel series of optically active photochromic (meth)acrylic homopolymers characterized by the presence in the side-chain of each repeating unit of a chiral centre of one single absolute configuration based on a L-lactic acid residue and the *trans*-4-aminoazobenzene moiety [1]. The above structural features allow to design macromolecules having the maximum content of chiral repeating units accompanied by the closest vicinity among the photochromic chromophores, thus favouring cooperative dipole–dipole interactions along the backbone among the azobenzene moieties disposed in a dissymmetric arrangement of a prevailing handedness. This conformational situation may be readily evidenced in the circular dichroism (CD) spectra of the polymers by the occurrence of a strong exciton couplet connected with the $\pi \rightarrow \pi^*$ electronic transition of the azobenzene chromophore in the *trans* configuration. Indeed, poly[(S)-4-(2-methacryloyloxypropanoylamino)azobenzene] [poly(**MLA**)] and poly[(S)-4-(2-acryloyloxypropanoylamino)azobenzene] [poly(**ALA**)], bearing the L-lactic acid moiety interposed between the main chain and the *trans*-4-aminoazobenzene group (Chart 1), showed CD couplets of appreciable amplitude, attributed to an ordered conformational arrangement of the macromolecules with a prevailing chirality [1]. More recently [2], we reported the synthesis of poly[(S)-4-(2-methacryloyloxypropanoyloxy)azobenzene] [poly(**MLO**)], having the L-lactic residue linked between the backbone and the *trans*-4-hydroxyazobenzene moiety (Chart 1). This polymer exhibited an intense CD couplet in correspondence of the $\pi \rightarrow \pi^*$ electronic transition of the *trans*-azobenzene chromophore, but with a large asymmetry, thus suggesting a lower conformational homogeneity of the macromolecules, as compared with poly(**MLA**), where an amido group able to give hydrogen bonds, is present between the chiral centre and the azobenzene moiety.

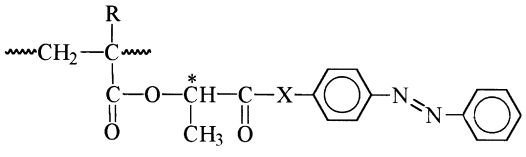

poly(**ALA**) (R = H, X = NH)
poly(**MLA**) (R = CH_3, X = NH)
poly(**MLO**) (R = CH_3, X = O)

Chart 1

* Corresponding author. Tel.: +39-50-918-226; fax: +39-50-918-260.
E-mail address: carlini@dcci.unipi.it (C. Carlini).

0032-3861/00/$ - see front matter
PII: S0032-3861(99)00701-6

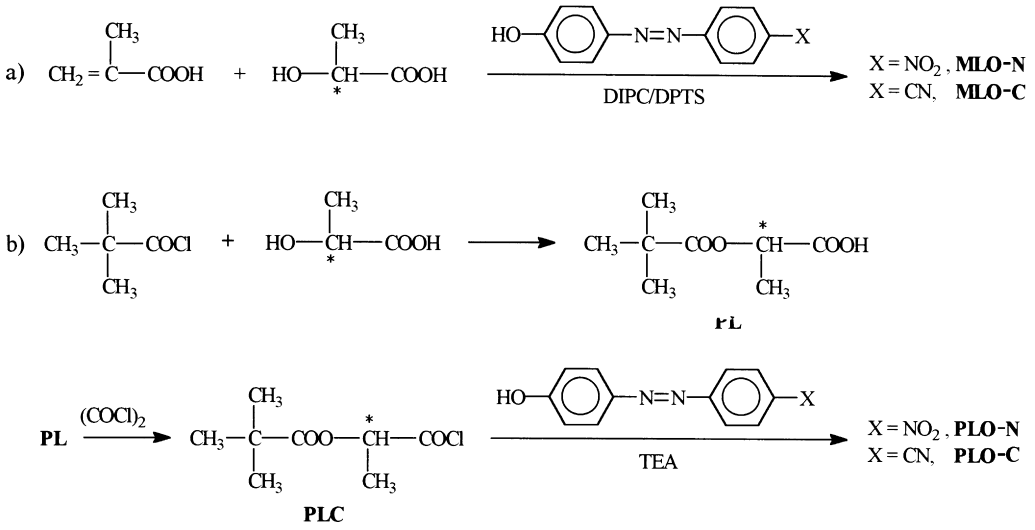

Scheme 1.

However, the high amplitude of this couplet allowed to conclude that, at least for sections, the macromolecules still assume an ordered conformational arrangement of a predominant chirality. Indeed, the disappearance of the CD couplet upon *trans–cis* photoisomerization and the contemporary appearance of a rather intense single CD band at the photostationary state, seemed to confirm the above hypothesis [2]. Finally, we described the synthesis of the homopolymer of *trans*-(S)-4-(2-methacryloyloxypropanoyloxy)-4′-formylazobenzene [poly(**MLO-F**)] (Chart 2), in order to study the effect on the chiroptical properties of the macromolecules by an electron-withdrawing moiety in the *para*-position of the azobenzene chromophore [3], the obtained results indicating that poly(**MLO-F**) macromolecules exist in a prevailing one-handed dissymmetric conformation, quite similar to that previously observed for poly(**MLO**).

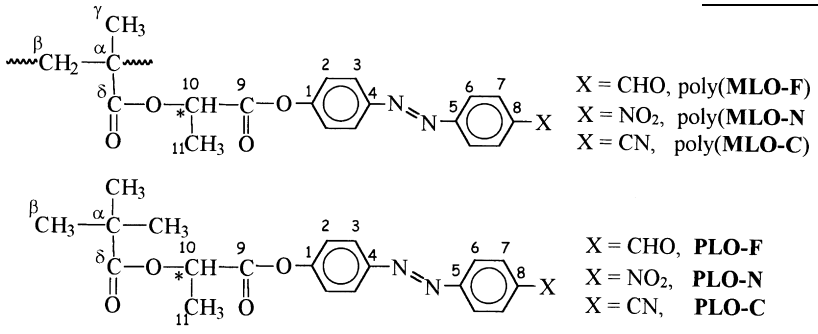

Chart 2

In this context, it appeared of interest to synthesize novel methacrylic homopolymers based on L-lactic acid connected to *trans*-azobenzene chromophores bearing in the 4′-position stronger electron-withdrawing moieties, such as nitro and cyano groups, able to increase the polarization of the photochromic system and in principle their dipole–dipole interaction along the macromolecules.

Therefore, this paper deals with the synthesis, structural characterization and chiroptical properties of poly[(S)-4-(2-methacryloyloxypropanoyloxy)-4′-nitroazo- benzene] and poly[(S)-4-(2-methacryloyloxypropanoyloxy)-4′-cyanoazobenzene] in the *trans* configuration [poly(**MLO-N**) and poly(**MLO-C**), respectively] and their comparison with poly(**MLO-F**) as well as with the corresponding low molecular weight models, such as *trans*-(S)-4-(2-pivaloyloxypropanoyloxy)-4′-formylazobenzene (**PLO-F**), *trans*-(S)-4-(2-pivaloyloxypropanoyloxy)-4′-nitroazobenzene (**PLO-N**) and *trans*-(S)-4-(2-pivaloyloxypropanoyloxy)-4′-cyanoazobenzene (**PLO-C**) (Chart 2). Finally, the photochromic behaviour of the above polymers has also been studied.

To this regard, these polymeric systems could also be of interest as materials potentially suitable for reversible optical storage, chemical photoreceptors and more in general for non-linear optical applications [4].

2. Experimental

2.1. Chemicals

(+)-L-Lactic acid (Aldrich) was purified by distillation (b.p. 99°C/0.2 mbar) in order to remove L-lactide and anhydride impurities [5], $[\alpha]_D^{25} = +3.7$ ($c = 5$, H_2O) (lit. [6]:

Table 1
Optical activity data and reaction yields for monomers and corresponding structural model compounds

Sample	Yield (mol%)	$[\alpha]_D^{25}$ [a]	$[\Phi]_D^{25}$ [b]
MLO-F[c]	21[d]	−15.4	−56.5
MLO-C	17[d]	−15.6	−56.4
MLO-N	17[d]	−16.9	−64.7
PLO-F[c]	23[e]	−40.9	−156.2
PLO-C	31[e]	−43.1	−163.3
PLO-N	21[e]	−39.1	−155.9

[a] Specific rotatory power in $CHCl_3$ solution.
[b] Molar rotatory power, calculated as: $([\alpha]_D^{25} \times M)/100$, where M represents the molecular weight of the sample or of the repeating unit, in the case of polymers.
[c] Ref. [3].
[d] Evaluated with respect to L-lactic acid.
[e] Evaluated with respect to **PL**.

$[\alpha]_D^{15} = +3.8$ ($c = 10.5$, H_2O). Triethylamine (**TEA**) (Aldrich) was refluxed on anhydrous $CaCl_2$ for 8 h and then distilled under dry nitrogen (b.p. = 89°C). Methacryloyl chloride (Aldrich) was distilled under dry nitrogen in the presence of traces of 2,6-di-*tert*-butyl-*p*-cresol as polymerization inhibitor just before use. Pivaloyl chloride (Aldrich) was distilled under dry nitrogen just before use. Methacrylic acid, 1,3-di*iso*propylcarbodiimide (DIPC) and 4-dimethylaminopyridine (Aldrich) were used as received. 4-Dimethylaminopyridinium 4-toluensulfonate (DPTS) was prepared from 4-dimethylaminopyridine and 4-toluensulfonic acid [7]. Methacryloyl-L-lactic acid (**ML**), having $[\alpha]_D^{25} - 28.0$ ($c = 1$, EtOH), was prepared as previously described [3]. *trans*-4-(4-Hydroxyphenylazo)benzaldehyde (**HA-F**) (m.p. = 197°C, lit. [8]: m.p. = 199°C) was prepared in 78% yield by coupling the diazonium salt of 4-aminobenzaldehyde with phenol, as previously reported [3]. *trans*-4-(4-Hydroxyphenylazo)benzonitrile (**HA-C**) (m.p. = 202°C, lit. [9]: m.p. = 203°C) was prepared in 80% yield by diazotation of 4-aminobenzonitrile followed by the coupling of the resulting diazonium salt with phenol, as previously described [9]. *trans*-4-(4-Hydroxyphenylazo)-nitrobenzene (**HA-N**) (m.p. = 211°C, according to the literature [10]) was synthesized [10,11] in 76% yield, starting from 4-nitroaniline and phenol, with the same procedure as reported for **HA-C**.

2.2. Monomers

trans-(S)-4-(2-Methacryloyloxypropanoyloxy)-4′-formyl-azobenzene (**MLO-F**) was prepared as previously reported [3] {$[\alpha]_D^{25} = -15.4$ ($c = 0.26$, $CHCl_3$), m.p. = 92°C}. *trans*-(S)-4-(2-Methacryloyloxypropanoyloxy)-4′-cyanoazobenzene (**MLO-C**) and *trans*-(S)-4-(2-methacryloyloxypropanoyloxy)-4′-nitroazobenzene (**MLO-N**) were prepared according to a general procedure [7] consisting of the one-pot reaction of methacrylic acid, L-lactic acid, and the appropriate 4-hydroxyazobenzene derivative (**HA-C** or **HA-N**) in the presence of DIPC and DPTS as coupling agent and condensation activator, respectively (Scheme 1a). Optical activity data and reaction yields are reported in Table 1.

As an example, the synthesis of **MLO-C** is reported below in detail.

In a 250 ml three-necked round-bottomed flask, under dry nitrogen, 44.4 mmol of L-lactic acid, 44.4 mmol of methacrylic acid and 0.5 g of hydroquinone as polymerization inhibitor, were introduced and dissolved in 100 ml of CH_2Cl_2 under magnetic stirring. Then, 48.8 mmol of **HA-C**, 44.4 mmol of DPTS and 115 mmol of DIPC were added and the resulting solution was maintained under vigorous stirring at room temperature for 72 h. The reaction mixture, after filtration for removing *N*,*N*-diisopropylurea thus formed, was treated with several portions of aq. 1 M HCl, 5% aq. Na_2CO_3 and water, in that order. The organic layer was dried over anhydrous Na_2SO_4 and the solvent removed under vacuum to dryness. The crude solid product was eluted on silica gel with chloroform to give 7.4 mmol of pure **MLO-C** (17% yield) {$[\alpha]_D^{25} = -15.6$ ($c = 0.21$, $CHCl_3$), m.p. = 78°C}.

^{1}H NMR ($CDCl_3$): $\delta = 8.0$–7.8 (m; 6H, aromatic protons), 7.4 (dd; 2H, aromatic protons in *ortho*-position to –O–CO– group), 6.3 and 5.7 (2d; 2H, CH_2=), 5.3 (q; 1H, CH–), 2.0 (s; 3H, CH_3–C=), 1.7 (d; 3H, CH_3–CH–).

FT-IR (KBr): 3066 (ν_{CH}, aromatic), 2983 (ν_{CH}, aliphatic), 2232 (ν_{CN}), 1784 ($\nu_{C=O}$, aromatic ester), 1729 ($\nu_{C=O}$, methacrylic ester), 1637 ($\nu_{C=C}$, methacrylic), 1594 ($\nu_{C=C}$, aromatic), 1454 ($\delta_{CH_{as}}$, CH_3), 1380 (δ_{CH_s}, CH_3), 850 (δ_{CH} 1,4-disubstituted phenyl rings) cm^{-1}.

Pure **MLO-N** was analogously obtained in 17% yield {$[\alpha]_D^{25} = -16.9$ ($c = 0.27$, $CHCl_3$), m.p. = 87°C}.

^{1}H NMR ($CDCl_3$): $\delta = 8.4$ (dd; 2H, aromatic protons in *ortho*-position to $-NO_2$), 8.1 (m; 4H, aromatic protons in *ortho*-position to the azo group), 7.3 (dd; 2H, aromatic protons in *ortho*-position to –O–CO– group), 6.3 and 5.7 (2d; 2H, CH_2=), 5.3 (q; 1H, CH–), 2.0 (s; 3H, CH_3–C=), 1.7 (d; 3H, CH_3–CH–).

FT-IR (KBr): 3080 (ν_{CH}, aromatic), 2932 (ν_{CH}, aliphatic), 1773 ($\nu_{C=O}$, aromatic ester), 1719 ($\nu_{C=O}$, methacrylic ester), 1636 ($\nu_{C=C}$, methacrylic), 1608 ($\nu_{C=C}$, aromatic), 1531 (ν_{NO_2as}), 1455 ($\delta_{CH_{as}}$, CH_3), 1381 (δ_{CH_s}, CH_3), 1348 (ν_{NO_2s}), 867 (δ_{CH} 1,4-disubstituted phenyl rings) cm^{-1}.

2.3. Low molecular weight structural models

trans-(S)-4-(2-Pivaloyloxypropanoyloxy)-4′-cyano-azobenzene (**PLO-C**) and *trans*-(S)-4-(2-pivaloyloxypropanoyloxy)-4′-nitro-azobenzene (**PLO-N**) were prepared according to a general procedure which involves firstly the reaction of pivaloyl chloride with L-lactic acid to give [1] pivaloyl-L-lactic acid (**PL**) {$[\alpha]_D^{25} = -43.4$ ($c = 1$, EtOH), m.p. = 61°C, 78% yield}, followed by chlorination with oxalyl chloride to afford pivaloyl L-lactic acid chloride (**PLC**), which is directly reacted with the appropriate 4-hydroxyazobenzene derivative to give the desired model

Table 2
Characterization of poly(**MLO-C**) and poly(**MLO-N**), as compared with poly(**MLO-F**) (polymerization conditions: see Section 2)

Polymer	Yield (%)[a]	$\overline{M}_n$[b]	$\overline{M}_w/\overline{M}_n$[b]	$[\alpha]_D^{25}$[c]	$[\Phi]_D^{25}$[d]	T_g (°C)[e]	C_p (J g^{-1} K^{-1})[e,f]	T_d (°C)[g]
Poly(**MLO-C**)	77	16 500	1.3	−143	−520	134	0.22	270
Poly(**MLO-N**)	75	10 500	1.5	−133	−510	134	0.24	255
Poly(**MLO-F**)[h]	76	46 000	2.4	−157	−575	98	0.18	225

[a] Evaluated as: (wt. of polymer/wt. of monomer) × 100.
[b] Determined by SEC analysis.
[c] Specific rotatory power.
[d] Molar rotatory power.
[e] Determined by DSC analysis.
[f] Specific heat capacity change at T_g.
[g] Initial decomposition temperature, determined by TGA analysis.
[h] Ref. [3].

compound (Scheme 1b). Optical activity data and reaction yields are reported in Table 1.

As an example the synthesis of **PLO-C** is reported below in detail.

Chlorination of pivaloyl-L-lactic acid (**PL**) by oxalyl chloride to give the corresponding acyl chloride **PLC**.

In a 100 ml three-necked round-bottomed flask, equipped with a dropping funnel and a condenser, under dry nitrogen, 46.9 mmol of oxalyl chloride were added dropwise at room temperature to 31.9 mmol of **PL** under vigorous stirring. The reaction mixture was left at room temperature for 2 h, then heated at 40°C for further 2 h until complete disappearance of the IR band at 1760 cm^{-1}, related to ν_{CO} of the **PL** carboxylic group, occurred. Then, excess oxalyl chloride was removed by adding anhydrous benzene and subsequent distillation to dryness under vacuum. **PLC** was thus obtained as a solid residue.

Reaction of **PLC** with *trans*-4-(4-hydroxyphenylazo)-benzonitrile (**HA-C**) to yield **PLO-C**.

In a 100 ml three-necked round-bottomed flask, equipped with a dropping funnel and a condenser, under dry nitrogen, a **PLC** (6.3 mmol) solution in anhydrous THF was added dropwise at room temperature to 6.3 mmol of **HA-C** dissolved in 8 ml of anhydrous THF. Then, 12.7 mmol of **TEA** were added dropwise to the reaction mixture at room temperature. A precipitate of triethylammonium chloride was immediately observed. The reaction mixture was left at room temperature for two days and after filtration treated with an equal volume of $CHCl_3$, washed with aq. 1 M HCl, 5% aq. Na_2CO_3 and finally with water. The organic layer was dried over anhydrous Na_2SO_4 and evaporated to dryness under vacuum. The crude solid product was crystallized from EtOH/H_2O (1:1, v/v) and then eluted on silica gel with chloroform to afford pure **PLO-C** in 31% yield {$[\alpha]_D^{25} = -46.1$ ($c = 0.21$, $CHCl_3$), m.p. = 116°C}.

^{1}H NMR ($CDCl_3$) (see Structure 2 for protons numbering): $\delta = 7.92$ (m, $J_{2,3}$ 8.94 Hz, 2H, CH-3), 7.88 (m; $J_{6,7}$ 8.57 Hz, 2H, CH-6), 7.72 (m; 2H, CH-7), 7.24 (m; 2H, CH-2), 5.22 (q; $J_{10,11}$ 11.2 Hz, 1H, CH-10), 1.65 (d; 3H, CH_3-11), 1.25 (s; 9H, CH_3-β).

FT-IR (KBr): 3065 (ν_{CH}, aromatic), 2982 (ν_{CH}, aliphatic), 2232 (ν_{CN}), 1786 ($\nu_{C=O}$, aromatic ester), 1739 ($\nu_{C=O}$, aliphatic ester), 1594 ($\nu_{C=C}$, aromatic), 1379 and 1369 (δ_{CH}, gem-dimethyl groups in *tert*-butyl moiety), 851 (δ_{CH}, 1,4-disubstituted phenyl rings) cm^{-1}.

2D HECTOR ($CDCl_3$): cross peaks between signals at about 16 and 1,3, 27 and 1,7, 68 and 5,2, 122 and 7,2, 133 and 7,7, 122 and 7,9, 123 and 7,9 ppm in the ^{13}C NMR and ^{1}H NMR spectrum, respectively.

Pure **PLO-N** was analogously obtained in 21% yield {$[\alpha]_D^{25} = -39.1$ ($c = 0.28$, $CHCl_3$); m.p. = 121°C}.

^{1}H NMR ($CDCl_3$) (see Chart 2 for protons numbering): $\delta = 8.3$ (d; $J_{6,7}$ 8.84 Hz, 2H, CH-7), 7.95 (m; 4H, CH-3 and CH-6), 7.28 (d; $J_{2,3}$ 8.71 Hz, 2H, CH-2), 5.23 (q; $J_{10,11}$ 7.08 Hz, 1H, CH-10), 1.65 (d; 3H, CH_3-11), 1.25 (s; 9H, CH_3-β).

FT-IR (KBr): 3075 (ν_{CH}, aromatic), 2964 (ν_{CH}, aliphatic), 1780 ($\nu_{C=O}$, aromatic ester), 1736 ($\nu_{C=O}$, aliphatic ester), 1592 ($\nu_{C=C}$, aromatic), 1518 (ν_{NO_2as}), 1342 (ν_{NO_2s}), 1379 and 1365 (δ_{CH}, gem-dimethyl groups in *tert*-butyl moiety), 860 (δ_{CH}, 1,4-disubstituted phenyl rings) cm^{-1}.

2D HECTOR ($CDCl_3$): cross peaks between the signals at about 16 and 1,3, 27 and 1,7, 68 and 5,2, 122 and 7,2, 123 and 7,8, 125 and 8,3, 125 and 7,8 ppm in the ^{13}C NMR and ^{1}H NMR spectrum, respectively.

trans-(S)-4-(2-Pivaloyloxypropanoyloxy)-4′-formylazo-benzene (**PLO-F**), was obtained in 23% yield, as previously described according to the above procedure [3]. {$[\alpha]_D^{25} = -49.9$ ($c = 0.29$, $CHCl_3$); m.p. = 106.9°C}.

2D HECTOR ($CDCl_3$): cross peaks between signals at about 16 and 1,3, 27 and 1,7, 68 and 5,3, 122 and 7,2, 123 and 8,0, 124 and 8,0, 130 and 8,0, 191 and 10 ppm in the ^{13}C NMR and ^{1}H NMR spectrum, respectively.

2.4. Polymers

Homopolymerizations were carried out in glass vials using 2,2′-azobis*iso*butyronitrile (AIBN) (2 wt.% with respect to the monomer) as free radical initiator and THF as solvent. The reaction components (1 g of monomer in 10 ml of THF) were introduced into the vial under nitrogen, submitted to several freeze-thaw cycles, and allowed to

polymerize at 70°C for 120 h. The polymerization was stopped by pouring the reaction mixture into a large excess of petroleum ether. The coagulated polymer was filtered, redissolved in $CHCl_3$, precipitated again in methanol and finally dried under high vacuum. All the polymeric products were structurally characterized by ^{1}H-and ^{13}C NMR, FT-IR and SEC analyses. Glass transition temperature (T_g), and thermal stability properties were also determined. The most relevant data are reported in Table 2.

2.5. Physico-chemical measurements

NMR spectra were recorded at room temperature on 5–10% $CDCl_3$ solutions with a Varian Gemini 200 spectrometer. ^{1}H NMR spectra were performed at 200 MHz, by using the following experimental conditions: 11,968 data points, 3 kHz spectral width, 30° pulse, 2 s acquisition time, 1 transient. 2D COSY spectra were recorded at 200 MHz by using the following experimental conditions: 1024 data points, 1742 Hz spectral width, eight transients, 1.7 s delay. A total of 256 spectra were recorded in order to have 1742 Hz spectral width in the second dimension. Final spectra have been symmetrized. ^{13}C NMR spectra were recorded at 50.3 MHz, under full proton decoupling, by using the following experimental conditions: 23,936 data points, 15 kHz spectral width, 70° pulse, 0.8 s acquisition time, 44,000 transients. No weighing function was applied prior to Fourier transformation. The 2D HETCOR spectra were recorded at 50.3 MHz by using sweep width of 10 kHz and 2 k data points. A total of 256 spectra were used to provide the equivalent of a 1.6 kHz sweep width in the ^{1}H frequency dimension. ^{13}C T_1 measurements were performed at 50.5 MHz by using the π–τ–π/2 pulse sequence and the following experimental conditions: 23,936 data points, 15 kHz spectral width, 70° pulse, 0.8 s acquisition time, 1024 transients, 6 s delay between sequences, delay between pulses $\tau = 0.023$, 0.047, 0.094, 0.188, 0.375, 0.75, 1.5, 3.0 and 6.0 s. Chemical shifts are given in ppm from TMS.

Number average molecular weights of the polymers ($\overline{M}_n$) were determined by a HPLC Waters Millipore 590 apparatus, equipped with an injector Waters Model U6K, a size exclusion chromatography (SEC) column Toso Haas G4000HXL and an UV–VIS detector Perkin–Elmer Model LC-95, working at 254 nm. The calibration curve was obtained by using several monodisperse polystyrene standards.

FT-IR spectra were carried out on a Perkin–Elmer 1750 spectrophotometer, equipped with an Epson Endeavour II data station. The samples were prepared as KBr pellets or as liquid films interposed between KBr discs.

Optical activity experiments were accomplished at 25°C on a Jasco DIP-360 digital polarimeter, using a cell path length of 1 dm. Specific rotatory powers at sodium D-line ($[\alpha]_D^{25}$) are expressed as 100° dm^{-1} g^{-1} dl. Molar optical rotations ($[\Phi]_D^{25}$), were determined as ($[\alpha]_D^{25} \times M$)/100, where M represents the molecular weight of the compound and of the repeating unit in the case of homopolymers.

UV absorption spectra of the samples were recorded at 25°C in $CHCl_3$ solution on a Perkin–Elmer Lambda 19 spectrophotometer. The spectral regions 550–400 and 400–250 nm were investigated by using cell path lengths of 1 and 0.1 cm, respectively. Concentrations of azobenzene chromophore about 1×10^{-3} and 5×10^{-4} mol l^{-1} were used. CD spectra of the samples were performed at 25°C on a Jasco 500 a dichrograph, in $CHCl_3$ and THF solution. The same spectral regions, cell path lengths and concentrations as for UV measurements were used. $\Delta\epsilon$ values, expressed in deg l mol^{-1} cm^{-1}, were calculated by the following equation: $\Delta\epsilon = [\Theta]/3300$, where the molar ellipticity $[\Theta]$ (in deg cm^2 dmol^{-1}) refers to one azobenzene chromophore.

Glass transition temperatures (T_g) of the polymer samples were measured by differential scanning calorimetry (DSC) with a Perkin–Elmer DSC-7 instrument adopting a temperature program consisting of three heating and two cooling ramps starting from room temperature (heating/cooling rate 10 K/min). Each sample was heated up to only 180°C in order to avoid thermal decomposition. The initial thermal decomposition temperature (T_d) was determined on the polymer samples with a Perkin–Elmer TGA-7 thermogravimetric analyzer by heating the samples in air at a rate of 20 K/min. Melting temperatures of the models were determined by a Linkham THM 600 hot stage connected to a Linkham TMS temperature controlling device. For all the samples melting points within 1°C range were detected, according to a high degree of purity. Checking of the liquid crystalline behaviour was carried out with an Olympus BHS POL polarizing microscope through crossed polarizers.

Photoisomerization experiments were carried out at 25°C on samples in chloroform solution (absorbance <0.1 at the irradiation wavelength) using the following experimental set-up: the emission from a 150 W high pressure Hg–Xe lamp, filtered by a 366 nm interference filter (Balzer) with a ±5 nm bandwidth, was guided by a 3 mm × 50 cm quartz fibre on top of a magnetically stirred solution of the sample in a 10 mm quartz cell placed within the UV spectrophotometer. The isomerization kinetics were monitored by measuring the 320 nm absorbance every 10 s until the photostationary state was reached.

3. Results and discussion

3.1. Synthesis and structural characterization of low and high molecular weight azobenzene derivatives

trans-(S)-4-(2-Methacryloyloxypropanoyloxy)-4′-formylazobenzene (**MLO-F**) was obtained [3] with a procedure involving the synthesis of methacryloyl-L-lactic acid

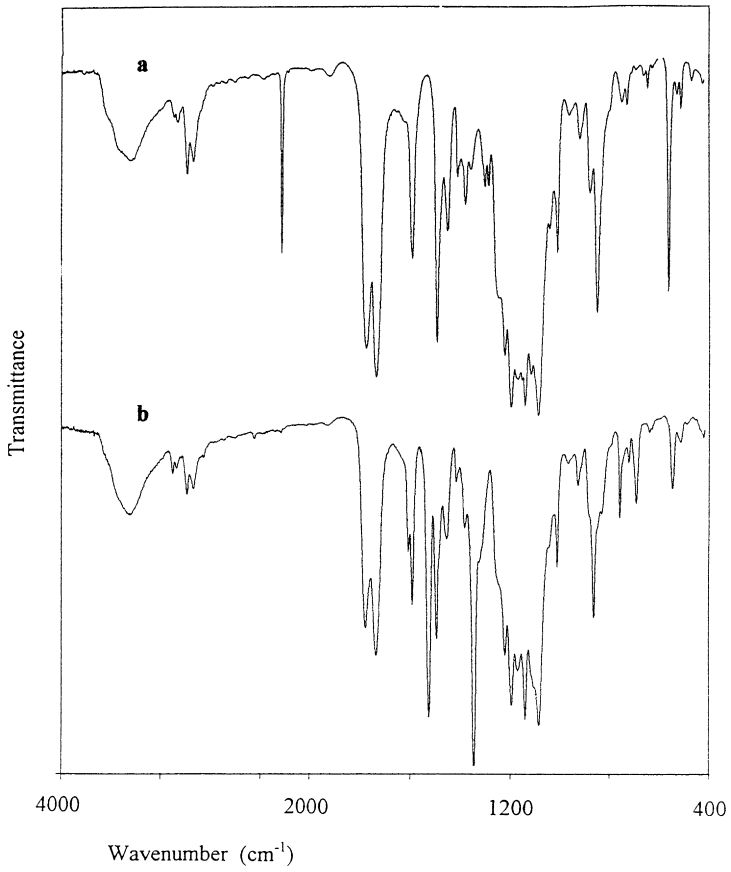

Fig. 1. FT-IR spectra of poly(**MLO-C**) (a) and poly(**MLO-N**) (b).

(**ML**) and its subsequent reaction with *trans*-4-(4-hydroxyphenylazo)benzaldehyde (**HA-F**) in the presence of 1,3-di*iso*propylcarbodiimide (DIPC) and 4-dimethylaminopyridinium 4-toluensulfonate (DPTS) as coupling agent and condensation activator, respectively, whereas *trans*-(S)-4-(2-methacryloyloxypropanoyloxy)-4′-nitroazobenzene (**MLO-N**) and *trans*-(S)-4-(2-methacryloyloxypropanoyloxy)-4′-cyanoazobenzene (**MLO-C**) were prepared by an one-pot reaction involving equimolar amounts of methacrylic acid, L-lactic acid and a slight excess of either *trans*-4-(4-hydroxyphenylazo)nitrobenzene (**HA-N**) or *trans*-4-(4-hydroxyphenylazo)benzonitrile (**HA-C**), in the presence of DIPC and DPTS, as previously described [2] for the synthesis of (S)-4-(2-methacryloyloxypropanoyloxy)-azobenzene (**MLO**) (Scheme 1a).

It was in fact proved [2] for **MLO** that the two procedures are substantially equivalent, the same mixture of products, containing about 20 mol% of the target monomer, being formed in both cases. Therefore, the one-pot reaction was preferred, due to greater simplicity of the procedure. Considering the successful application of this method to the synthesis of optically active polyesters starting from chiral hydroxy acid monomers [7], and the very mild conditions adopted (room temperature and non-protic apolar solvents), no racemization should occur during the reaction. A confirmation to this hypothesis comes from the fact that the samples of **MLO** prepared by the two different methods showed [2] the same specific rotation. Therefore, **MLO-N** and **MLO-C** have been assumed to be as optically pure as the L-lactic acid precursor (Table 1).

The low molecular weight models *trans*-(S)-4-(2-pivaloyloxypropanoyloxy)-4′-cyano-azobenzene (**PLO-C**) and *trans*-(S)-4-(2-pivaloyloxypropanoyloxy)-4′-nitro-azobenzene (**PLO-N**) were synthesized by a different synthetic pathway with respect to the corresponding monomers, as previously described [2,3] for the synthesis of (S)-4-(2-pivaloyloxypropanoyloxy)azobenzene (**PLO**) and **PLO-F** (Scheme 1b). The above procedure consists of the synthesis of the precursor pivaloyl L-lactic acid chloride (**PLC**), readily obtained by reacting pivaloyl-L-lactic acid (**PL**) with oxalyl chloride (contrary to what occurred for **ML**), followed by the reaction with either **HA-C** or **HA-N**, in the presence of triethylamine. Also in this case no racemization should occur under the adopted mild conditions and therefore **PLO-N** and **PLO-C** have been also assumed to be as optically pure as the L-lactic acid precursor (Table 1).

Poly(**MLO-C**) and poly(**MLO-N**) were prepared by free radical initiation in the presence of a rather large amount (2 wt.%) of **AIBN**, due to the well known low reactivity of unsaturated monomers bearing an azoaromatic group [12,13]. Under these conditions and by using a quite long polymerization time, the polymers were obtained in rather

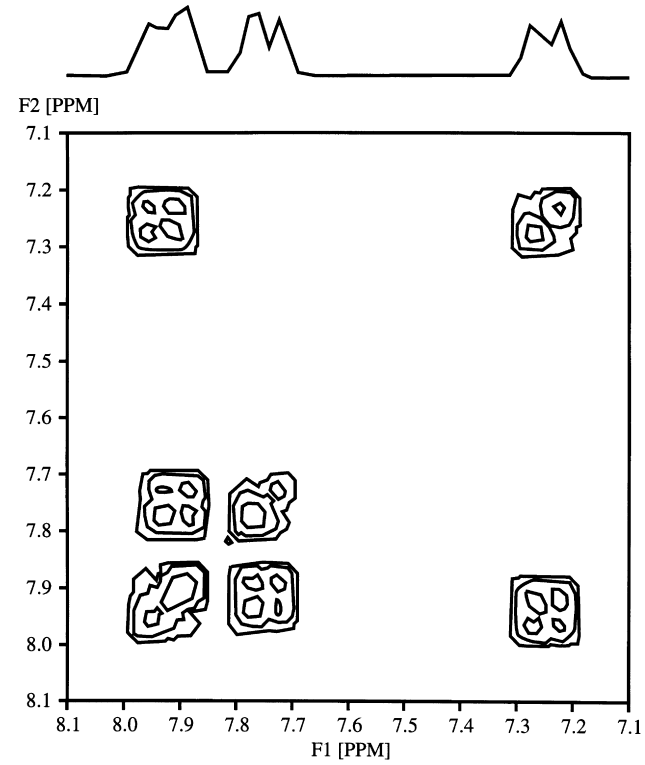

Fig. 2. Aromatic proton region of the 2D COSY NMR spectrum of **PLO-C** in $CDCl_3$ solution.

high yield (76%), substantially the same as that reported for poly(**MLO**) [2] and poly(**MLO-F**) [3] (Table 2). The average molecular weights resulted appreciably lower (Table 2) than those observed for poly(**MLO**) and poly(**MLO-F**), thus suggesting that cyano- and nitro-substituted azobenzene chromophores favour chain transfer reactions during the polymerization. The polydispersity of the polymers is typical of a free radical polymerization process, as evidenced by $\overline{M}_w/\overline{M}_n$ values (Table 2).

The IR analysis of the polymers confirms the expected structures (Fig. 1). Indeed poly(**MLO-C**) and poly(**MLO-N**) do not show the band around 1636 cm^{-1}, related to C=C stretching vibration of the methacrylic group, present in the corresponding monomers. Moreover, they retain, respectively, the bands at 2229 cm^{-1}, attributable to the C–N stretching vibration of the cyano group [14], as well as those at 1525 and 1345 cm^{-1}, typical of the asymmetric and symmetric modes of N=O stretching vibration of the nitro group [14]. Finally, the band present in poly(**MLO-C**) and poly(**MLO-N**) at about 1735 cm^{-1}, connected with the stretching vibration of aliphatic C=O ester group, results shifted towards higher frequencies, as compared with the corresponding monomers, by about 7 and 16 cm^{-1}, respectively, according to a lower electronic delocalization in the polymer samples due to the disappearance of the methacrylic double bond. Accordingly, an analogous shift was observed for **PLO-C** and **PLO-N** models. Similar results were previously observed in methacrylic and acrylic polymers bearing side-chain azoaromatic moieties [1–3,13].

In order to have a better insight on the molecular structure and main chain stereoregularity, the polymers were also investigated by ^1H- and ^{13}C NMR in comparison with the corresponding models. The aromatic region of ^1H NMR spectra of both polymer samples and low molecular weight model compounds is characterized by the presence of two or three groups of peaks. In order to unequivocally attribute these signals, a 2D-NMR COSY investigation of **PLO-C** and **PLO-N** was undertaken. The off-diagonal resonances in the aromatic proton region of **PLO-C** (Fig. 2) evidenced a coupling between the signal at 7.2 and 7.9 ppm. Therefore, on the basis of their coupling constants, the signals at 7.24, 7.72, 7.88 and 7.92 ppm must be attributed to the aromatic protons bonded to C-2, C-7, C-6 and C-3 respectively (Chart 2), that is the most deshielded protons are those in *meta* position to the ester group.

Due to inductive effects provided by the substituents of the azobenzene chromophore, C-3 protons would be expected to experience a smaller deshielding effect than those present in the cyano-substituted aromatic ring, containing two electron-withdrawing groups. The experimental results seem therefore to indicate a significant contribution by internal charge transfer mesomers to the electronic distribution of the 4-oxy-4′-cyano-azobenzene chromophore [15,16] as shown in Chart 3.

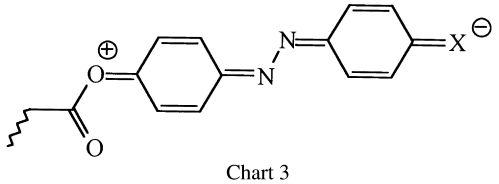

Chart 3

The overlap of C-3, C-6, and C-7 proton signals is in agreement with the occurrence of a similar phenomenon in both **PLO-F** and poly(**MLO-F**) [3].

The off-diagonal resonances in the aromatic proton region of **PLO-N** COSY spectrum (Fig. 3) evidenced a coupling between signals at 7.3 and 8.0 ppm. Therefore signals at about 7.3, 8.0 and 8.3 ppm must be attributed to the aromatic protons bonded to C-2, C-3 and C-6 (overlapped), and C-7, respectively (Chart 2). Also in this case, the overlap of C-3 and C-6 proton signals suggests the occurrence of a contribution from internal charge transfer mesomers. However, the large downfield shift of the C-7 proton indicates that in the case of the nitro substituent, inductive effects prevail on mesomeric ones.

Attribution of the signals present in the ^{13}C NMR spectra of the investigated polymer samples (Table 3) were performed on the basis of 2D HETCOR spectra, additive group contributions [17], relative intensity and multiplicity in undecoupled spectra.

The 2D HETCOR spectra of **PLO-N** (Fig. 4) as well as of **PLO-C** and **PLO-F** showed cross peaks between the signals

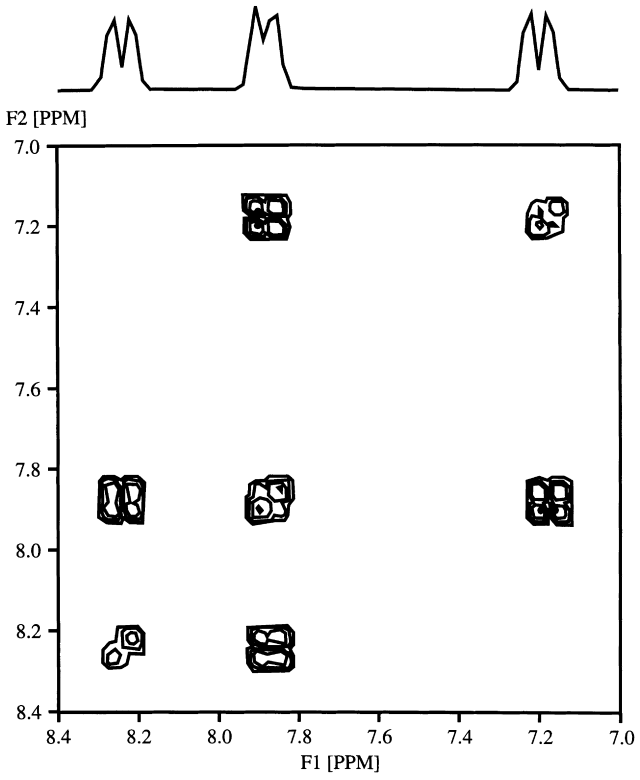

Fig. 3. Aromatic proton region of the 2D COSY NMR spectrum of **PLO-N** in $CDCl_3$ solution.

in agreement with the ^{13}C- and ^{1}H NMR assignments reported in Table 3 and the experimental part, respectively. However, attributions of the signals of quaternary aromatic carbons, made only from group contributions, may be not entirely correct, due to the modification of the electron distribution on the azobenzene chromophore consequent the internal charge transfer process.

^{13}C NMR signals relevant to α-δ carbons of polymer samples appeared as partially overlapping multiplets, indicating their sensitivity to main chain stereochemistry. The overlap of C-γ and C-11 signals prevented careful evaluation of polymer tacticity. However the relative intensities of peak splittings, particularly those of C-δ signals [18,19], allowed to assign roughly a 70% content of syndiotactic dyads to the investigated polymer samples, by assuming a Bernoullian statistics [20].

To gain information on the polymer molecular mobility, ^{13}C NMR relaxation times (T_1) of polymer samples, and for comparison of model compounds, were measured at 50.3 MHz, in $CDCl_3$ solution at room temperature (Table 4). Correlation times (τ) were evaluated from the corresponding T_1 values, under the rather crude assumption that the relaxation mechanism is exclusively dipolar and that only directly bonded hydrogen atoms contribute to the relaxation process [17] (Table 4).

Model compound carbons, not taking into account quaternary ones, had τ values included between 0.9 and 5.2×10^{-11} s, evidencing an appreciable mobility of the low molecular weight molecules with some deviation from an isotropic overall tumbling model with a single correlation time. Moreover, the reported correlation times are almost one order of magnitude lower than those of typical low molecular weight compounds, in accordance with the rather extended and stiff structure of the investigated azobenzene derivatives.

T_1 values of the carbons of polymer samples are lower than those of the corresponding model compounds, in

Table 3
Assignments (see Chart 2) of the signals present in ^{13}C NMR spectra of polymers and the corresponding low molecular weight models in $CDCl_3$ solution at 25°C

Attribution	Sample					
	PLO-F δ (ppm)	poly(**MLO-F**) δ (ppm)	**PLO-C** δ (ppm)	poly(**MLO-C**) δ (ppm)	**PLO-N** δ (ppm)	poly(**MLO-N**) δ (ppm)
C_α	38.42	45.42–45.08	38.99	45.07–45.42	38.12	45.08–45.48
C_β	26.82	55–50	26.84	55–50	26.85	55–50
C_γ	–	20–16	–	20–16	–	20–16
C_δ	177.91	178–175	177.79	178–175	177.88	178–175
C_1	152.82	152.57	153.02	152.75	153.19	152.93
C_2	121.99	121.97	122.03	122.03	122.10	122.10
C_3	124.40	124.36	124.45	124.45	123.30	123.24
C_4	150.09	149.99	149.87	149.85	148.60	148.56
C_5	155.47	155.23	154.07	153.87	155.33	155.04
C_6	123.19	123.15	123.19	123.16	124.55	124.50
C_7	130.18	130.43	133.00	133.00	124.55	124.50
C_8	137.34	137.38	113.89	114.00	149.92	149.91
C_9	169.12	168.85	169.03	168.62	169.08	168.65
C_{10}	68.32	69.26	68.29	69.11	68.31	69.22
C_{11}	16.50	~16.6[a]	16.49	~16.6[a]	16.51	~16.6[a]
C_X	191.43	191.22	118.19	118.08	–	–

[a] This peak overlaps the C_γ signal.

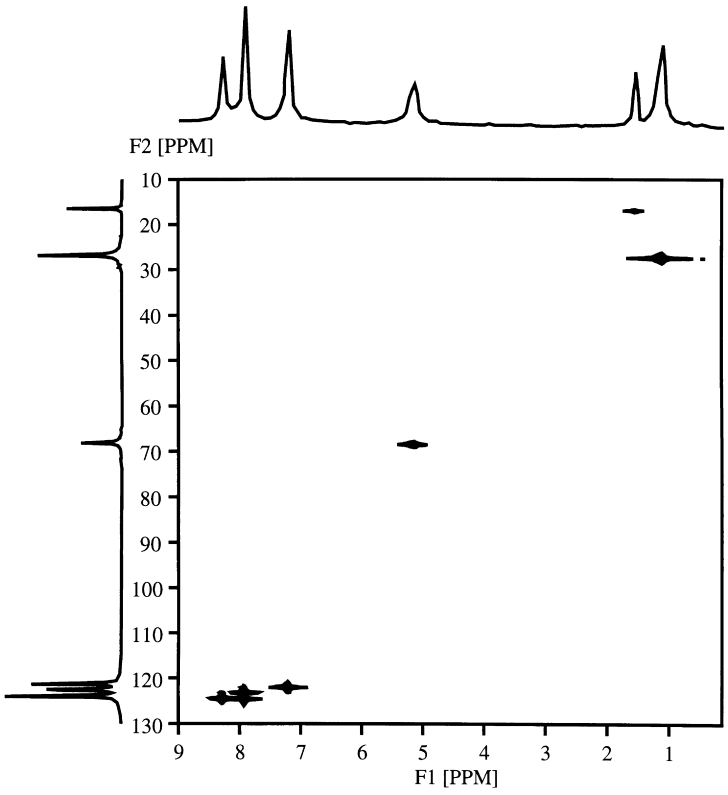

Fig. 4. 2D HETCOR NMR spectrum of **PLO-N** in $CDCl_3$ solution.

accordance with the reduced mobility of macromolecular systems. As expected, comparison of the different homopolymers does not highlight a significant influence of the azobenzene electron-withdrawing substituent on τ values.

Interestingly, T_1 values of both high and low molecular weight samples are 10–30% lower than those of the corresponding unsubstituted **PLO** and poly(**MLO**) samples [21]. This effect can be tentatively attributed to the presence

Table 4
Relaxation times (T_1) and correlation times (τ) of signals present in ^{13}C NMR spectra of polymers and the corresponding low molecular weight models in $CDCl_3$ solution at 25°C (correlation times evaluated from T_1 values by assuming that the only relaxation process is dipolar and that only directly bonded hydrogens contribute to the relaxation process)

Carbon atom	Sample											
	PLO-F		poly(**MLO-F**)		**PLO-C**		poly(**MLO-C**)		**PLO-N**		poly(**MLO-N**)	
	T_1 (s)	$\tau\cdot10^{11}$ (s)	T_1 (s)	$\tau\cdot10^{11}$ (s)	T_1 (s)	$\tau\cdot10^{11}$ (s)	T_1 (s)	$\tau\cdot10^{11}$ (s)	T_1 (s)	$\tau\cdot10^{11}$ (s)	T_1 (s)	$\tau\cdot10^{11}$ (s)
C_α	>21	n.d.	1.5	n.d.	>17	n.d.	1.2	n.d.	>21	n.d.	1.4	n.d.
C_β	1.8	0.9	0.21	11.8	1.8	0.9	0.11	23	1.8	0.9	0.08	60
C_γ	–	–	0.07	77	–	–	0.07	77	–	–	0.07	77
C_δ	>35	n.d.	4.0	n.d.	>20	n.d.	3.7	n.d.	>20	n.d.	3.9	n.d.
C_1	>22	n.d.	3.2	n.d.	>15	n.d.	2.5	n.d.	>15	n.d.	3.2	n.d.
C_2	1.2	3.8	0.30	16.1	1.2	3.9	0.31	15.6	1.4	3.4	0.28	17.4
C_3	1.2	3.8	0.29	16.7	1.2	3.9	0.31	15.6	1.6	3.0	0.43	11.1
C_4	>14	n.d.	2.7	n.d.	>15	n.d.	2.5	n.d.	>22	n.d.	4.4	n.d.
C_5	>21	n.d.	4.3	n.d.	>13	n.d.	3.3	n.d.	>20	n.d.	3.9	n.d.
C_6	1.4	3.4	0.48	9.9	1.4	3.3	0.50	9.5	1.5	3.2	0.37	12.9
C_7	1.4	3.4	0.48	9.9	1.4	3.3	0.50	9.5	1.5	3.2	0.37	12.9
C_8	>31	8.5	3.3	n.d.	>13	n.d.	3.6	n.d.	>15	n.d.	3.0	n.d.
C_9	>15	n.d.	2.5	n.d.	>17	n.d.	2.1	n.d.	>20	n.d.	2.7	n.d.
C_{10}	0.92	5.1	0.18	28.4	0.91	5.2	0.19	26.6	1.03	4.6	0.20	25.1
C_{11}	0.83	1.9	0.26	9.3	0.84	1.9	0.30	5.4	0.86	1.8	0.31	5.2
C_X	1.6	3.0	0.56	8.5	3.9	n.d.	1.0	n.d.	–	–	–	–

Table 5
UV absorption spectra in $CHCl_3$ and THF of polymers and related model compounds in all *trans* configuration (λ_{max} and ϵ_{max} are expressed in nm and l mol^{-1} cm^{-1}, respectively)

Sample	Solvent	$n \rightarrow \pi^*$ transition		$\pi \rightarrow \pi^*$ transition	
		λ_{max}	ϵ_{max}	λ_{max}	$\epsilon_{max} \times 10^{-3}$
poly(**MLO-C**)	$CHCl_3$	449	760	331	24.8
	THF	450	685	331	27.7
PLO-C	$CHCl_3$	445	1 015	332	29.3
	THF	452	1 240	329	27.2
poly(**MLO-N**)	$CHCl_3$	452	870	338	25.4
	THF	453	820	335	28.4
PLO-N	$CHCl_3$	454	900	340	28.0
	THF	454	840	340	27.9
poly(**MLO-F**)[a]	$CHCl_3$	454	775	333	26.4
	THF	454	735	333	27.4
PLO-F[a]	$CHCl_3$	449	940	335	27.7
	THF	450	955	334	26.5

[a] Ref. [3].

of the 4′-substituent and to dipolar interactions that reduce the azobenzene chromophore mobility.

None of the polymers displayed a liquid crystalline behaviour, as checked by a polarizing microscope through crossed polarizers. Analogously, DSC measurements did not reveal any mesomorphic transition. This is probably due to the stiffness of the spacer between main chain and side-chain azobenzene mesogens that prevents their organization in a mesophase. Poly(**MLO-C**) and poly(**MLO-N**) showed (Table 2) significantly higher T_g values, as compared with poly(**MLO-F**) [3], the specific heat capacity change in the process being also slightly larger for the former systems. This occurrence seems to suggest that the higher electron withdrawing power of cyano and nitro moieties with respect to formyl group causes a higher polarization of the substituted azobenzene chromophores, thus increasing inter- and/or intra-molecular interactions between the above moieties and hence decreasing the mobility of the macromolecules. Accordingly, poly(**MLO-C**) and poly(**MLO-N**) resulted more thermally stable, as shown by their higher initial decomposition temperature with respect to poly(**MLO-F**) (Table 2).

3.2. Photochromic and chiroptical properties

UV spectra in THF and $CHCl_3$ solution of poly(**MLO-C**) and poly(**MLO-N**), as well as of the corresponding models **PLO-C** and **PLO-N**, showed in the 250–550 nm region two bands centered around 335 and 450 nm, related to the $\pi \rightarrow \pi^*$ and $n \rightarrow \pi^*$ electronic transition of the azobenzene chromophore in *trans* configuration [22] (Table 5). As an example, in Fig. 5 the UV spectra of poly(**MLO-C**) and of **PLO-C** in $CHCl_3$ solution are reported. As expected, the absorption maxima are located at higher wavelengths with respect to the 4′-unsubstituted derivatives poly(**MLO**) and **PLO**, which exhibited λ_{max} values close to 320 and 440 nm for the same transitions [2], due to the presence of the electron withdrawing groups which induce conjugation in the azoaromatic system [11,22] to a larger extent. A more detailed examination of the spectra in $CHCl_3$ solution indicates a hypochromic effect of the polymers with respect to the corresponding models, as far as the $\pi \rightarrow \pi^*$ transition is concerned. An analogous trend was found [3] for poly(**MLO-F**) and its model **PLO-F** (Table 5). This may be addressed to the occurrence of electrostatic dipole–dipole interactions between neighbouring side-chain

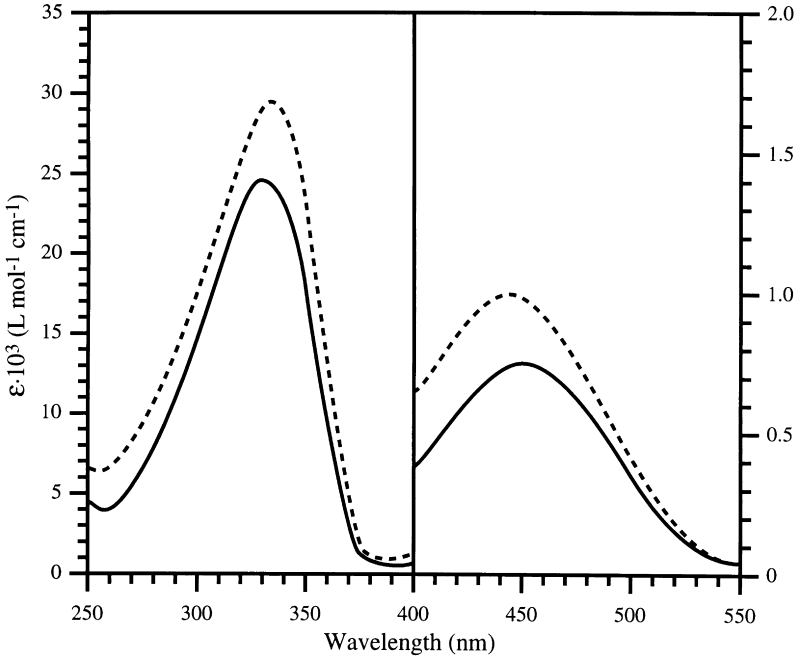

Fig. 5. UV spectra at 25°C of poly(**MLO-C**) (—) and **PLO-C** (– – –) in $CHCl_3$ solution.

Table 6
Photoisomerization kinetics of polymers and model compounds in chloroform solution at 25°C

Sample	$\kappa \times 10^5$ (s^{-1})	A_∞/A_0	Sample	$\kappa \times 10^5$ (s^{-1})	A_∞/A_0
PLO-C	7.9	0.24	poly(**MLO-C**)	6.7	0.45
PLO-F	12.5	0.53	poly(**MLO-F**)	11.4	0.70
PLO-N	20.4	0.93	poly(**MLO-N**)	28.1	0.93

aromatic moieties along the backbone [23,24] as previously observed in several polymeric systems with side-chain aromatic [25,26] and azoaromatic chromophores [1,2,13].

However, when the UV spectra were recorded in THF solution no hypochromic effect was observed in the polymers as compared with their models (Table 5). An analogous trend was found for poly(**MLO-F**) with respect to **PLO-F** [3]. This occurrence seems to suggest that the solvent polarity (the dielectric constants of THF and $CHCl_3$ at 25°C are 7.4 and 4.64 D, respectively [27]) can affect the interchromophore dipolar interactions and probably influence the conformational arrangement of the macromolecules. This hypothesis is confirmed by the fact that poly(**MLA**) and poly(**ALA**), containing aromatic amide groups in the side chains, showed [1] a remarkable hypochromic effect as compared with the corresponding low molecular weight structural models regardless of the use of THF or $CHCl_3$ as solvent, thus suggesting that their macromolecules are characterized by a more stable conformational arrangement, due to the occurrence of hydrogen bonds along the backbone.

Upon light irradiation at 366 nm, the azobenzene chromophores undergo a *trans* to *cis* photoisomerization process. Correspondingly, shape, intensity and position of the UV absorption bands are modified.

Photoisomerization kinetics were investigated at 25°C on chloroform solutions having absorbance lower than 0.1 at the irradiation wavelength. Experiments were performed by irradiating at 366 nm while monitoring the absorbance at 320 nm until a photostationary state was reached.

Kinetic data fitted the equation $\ln[(A_0 - A_\infty)/(A_t - A_\infty)] = \kappa \cdot t$, where A_0, A_t and A_∞ are the 320 nm absorbance at time 0, t and ∞, respectively [20]. In all cases experimental and calculated data were in very good agreement.

Taking into account that the evaluated photoisomerization rate constants linearly depend on the light intensity (I_{366}) at the irradiation wavelength [$\kappa = 2.303 \cdot I_{366}(\epsilon_{cis} \cdot \Phi_{cis} + \epsilon_{trans} \cdot \Phi_{trans})$] [21], the experimental values of kinetic constants (κ) were averaged over 2–4 experiments and corrected for the variation of I_{366}, as measured by a photodiode.

The rate constant values reported in Table 6 evidenced an appreciable influence of the azobenzene substituent on the photoisomerization kinetics, very likely due to the different electronic distribution of the aromatic chromophore. On the contrary, no significant difference was observed between polymers and the corresponding model compounds.

As expected, the rate constants are of the same order of magnitude as those of the unsubstituted azobenzene derivatives reported in a previous paper [2]. However, the A_∞/A_0 values are rather high, particularly in the case of nitro-substituted samples. This behavior has been tentatively attributed to a competition by the thermal *cis* to *trans* retro-isomerization process. To verify this hypothesis, the thermal *cis* to *trans* isomerization of a **PLO-N** sample at the photostationary state was investigated in $CHCl_3$ solution at 25°C. Indeed, the rate constant of this process resulted to be 23.7×10^{-5} s^{-1}, a value comparable to that of the *trans* to *cis* photoisomerization process.

All the polymers displayed in $CHCl_3$ solution a negative optical activity at sodium D-line as the corresponding monomers and structural models (Tables 1 and 2). However, the values of the molar rotatory power of the polymers are one order of magnitude higher with respect to the monomers and about four times higher as compared with the corresponding models, thus suggesting a higher conformational rigidity of the macromolecules. Moreover, poly(**MLO-C**) and poly(**MLO-N**), analogously to what found [3] for poly(**MLO-F**), displayed a higher molar rotatory power with respect to poly(**MLO**) [2], indicating that the presence of an electron withdrawing group on the 4′-position of the *trans*-azobenzene chromophores can improve the dissymmetry of the macromolecules. However, investigation of the chiroptical properties of the polymers by CD measurements in comparison with their low molecular weight model compounds allows a deeper insight on this point.

The CD spectra of poly(**MLO-C**) and poly(**MLO-N**), as well as those of the corresponding low molecular weight models **PLO-C** and **PLO-N**, exhibit both in $CHCl_3$ and THF solution (Table 7) a weak broad negative band in the 440-450 nm region, in close correspondence to the UV

Table 7
CD properties in $CHCl_3$ and THF solution at 25°C for poly(**MLO-C**) and poly(**MLO-N**), as compared with poly(**MLO-F**) and the corresponding structural models

Sample	Solvent	$n \rightarrow \pi^*$ transition		$\pi \rightarrow \pi^*$ transition			
		λ_1[a]	$\Delta\epsilon_1$[b]	λ_2[a]	$\Delta\epsilon_2$[b]	λ_3[a]	$\Delta\epsilon_3$[b]
poly(**MLO-C**)	$CHCl_3$	440	−0.21	343	−2.22	–	–
	THF	445	−0.13	343	−3.35	303	+0.44
PLO-C	$CHCl_3$	440	−0.12	330	−0.35	–	–
	THF	450	−0.09	330	−0.85	–	–
poly(**MLO-N**)	$CHCl_3$	451	−0.12	345	−1.52	–	–
	THF	450	−0.15	345	−2.24	–	–
PLO-N	$CHCl_3$	436	−0.16	331	−0.48	–	–
	THF	450	−0.05	335	−1.04	–	–
poly(**MLO-F**)[c]	$CHCl_3$	455	−0.20	346	−2.16	307	+0.40
	THF	452	−0.15	346	−3.03	307	+0.55
PLO-F[c]	$CHCl_3$	450	−0.05	335	−0.35	–	–
	THF	449	−0.05	335	−1.04	–	–

[a] Expressed in nm.
[b] Expressed in deg l mol^{-1} cm^{-1}.
[c] Ref. [3].

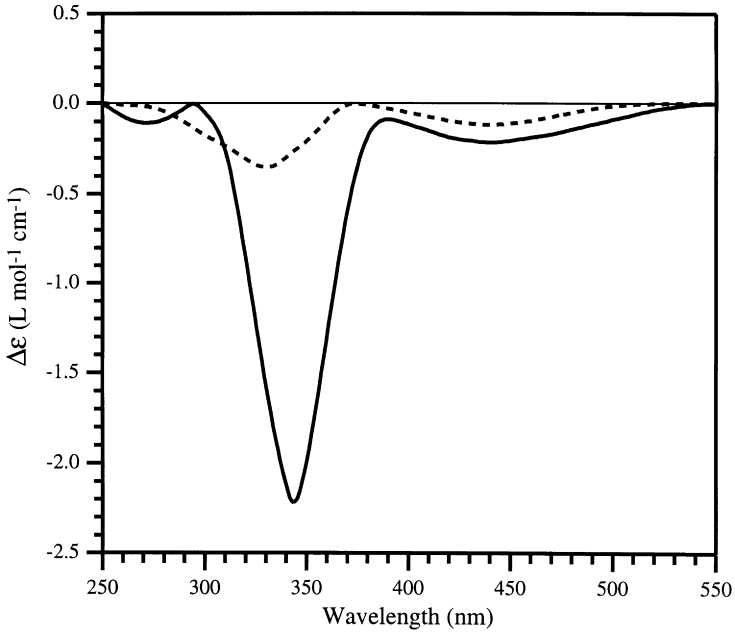

Fig. 6. CD spectra between 250 and 550 nm of poly(**MLO-C**) (—) and **PLO-C** (– – –) in $CHCl_3$ solution.

absorption related to the $n \rightarrow \pi^*$ electronic transition of the *trans*-azobenzene chromophore. An analogous result was obtained [3] for poly(**MLO-F**) and **PLO-F**, as reported in Table 7.

In the $\pi \rightarrow \pi^*$ spectral region poly(**MLO-C**) and poly(**MLO-N**) showed in $CHCl_3$ solution a single negative band much more intense than that of the corresponding models (Table 7 and Figs. 6 and 7).

However, in the case of these polymers, the maximum of the dichroic absorption is shifted to longer wavelengths with respect to the corresponding UV absorption. This behaviour is different from that reported for both poly(**MLO**) [2] and poly(**MLO-F**) [3] which displayed in the same region a CD couplet, although characterized by a large asymmetry. When THF was used as solvent, poly(**MLO-C**) displayed a splitting of the dichroic band in the $\pi \rightarrow \pi^*$ spectral region (Table 7 and Fig. 8), whereas poly(**MLO-N**) retained one single CD band of negative sign in the same region (Table 7 and Fig. 8). Indeed, poly(**MLO-C**) is characterized by the presence of two CD bands of opposite sign, located at 343 (negative) and 303 (positive) nm, shifted with respect to the corresponding UV maximum (331 nm) with a crossover

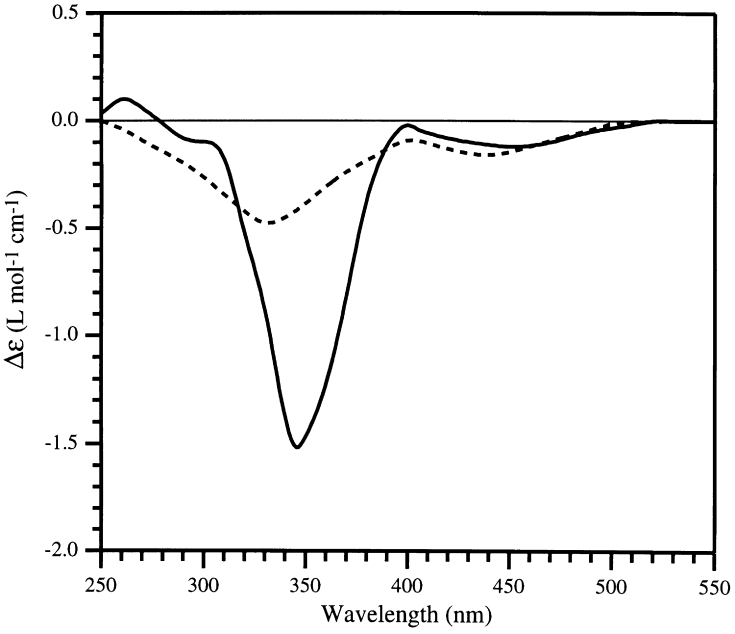

Fig. 7. CD spectra between 250 and 550 nm of poly(**MLO-N**) (—) and **PLO-N** (– – –) in $CHCl_3$ solution.

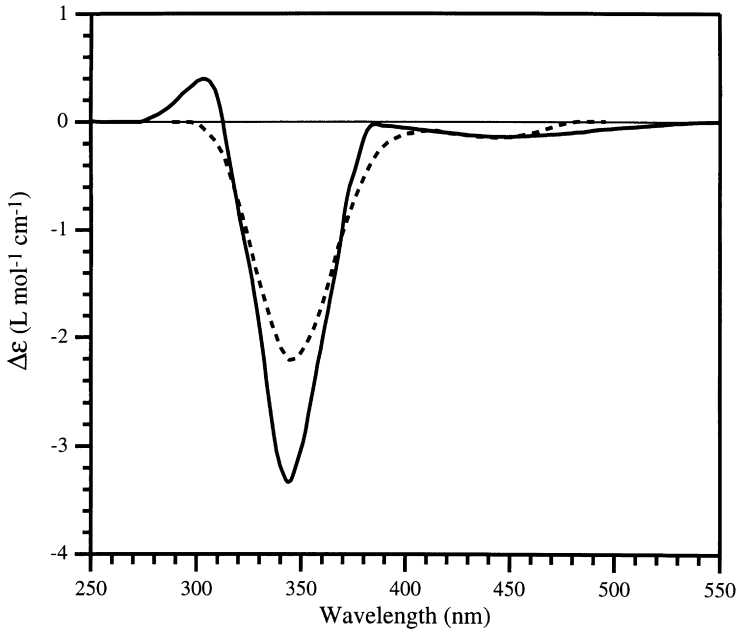

Fig. 8. CD spectra between 250 and 550 nm of poly(**MLO-C**) (—)and poly(**MLO-N**) (– – –) in THF solution.

point at 312 nm. In the case of poly(**MLO-N**), analogously to what observed in chloroform solution, the single CD band in THF solution is shifted towards longer wavelengths with respect to the UV absorption maximum.

All the above data seem to indicate that, on increasing the electron withdrawing character of the substituent in 4′-position (CHO < CN < NO_2) of side-chain azobenzene chromophores, the tendency of the polymers to give an exciton splitting of the CD band related to the $\pi \rightarrow \pi^*$ electronic transition is reduced. In this respect we have to consider that the presence of an electron withdrawing group in the 4′-position generates a permanent dipole along the major axis of the azobenzene chromophore with a dipole moment which increases in going from CHO to CN and NO_2, in that order. As permanent side-chain dipoles with the same polarization sense are present in the side chains, the electrostatic dipole–dipole repulsion between the neighbouring azobenzene groups could be responsible for the reduction or even the disappearance of the CD couplets. In fact, it may be suggested that as the polarization along the azobenzene chromophores increases, the repulsion between these moieties, and hence their interacting distance, also increases. This effect is allowed, or scarcely hindered, by the flexible L-lactic acid chiral moiety connecting the chromophore to the polymer backbone. On this basis, poly(**MLO-F**), where the formyl group is characterized by the lowest electron withdrawing power, can display CD couplets both in $CHCl_3$ and THF, although with a large asymmetry. Poly(**MLO-C**), where cyano groups have an intermediate electron withdrawing character, only in THF solution retains a CD couplet, absent in $CHCl_3$, due to the higher polarity and donor properties of the former solvent. Finally, poly(**MLO-N**), in which the nitro groups have the highest electron withdrawing character, does not show any CD couplet in either of the above solvents. However, the intense ellipticity of the single $\pi \rightarrow \pi^*$ dichroic bands as well as the large amplitude of the CD couplets, when present, as compared with the corresponding low molecular structural models, suggest that the above polymers are characterized by a significant dissymmetric arrangement of the macromolecules with one prevailing chirality, at least for chain sections.

It can be tentatively suggested that the electronic transitions related to the *trans*-azoaromatic chromophore (internal charge transfer and $\pi \rightarrow \pi^*$), which jointly contribute to the UV absorption band located at 335–340 nm (Table 5), could have a different sensitivity to the chiral geometry of the macromolecules, thus giving rise to slightly shifted dichroic bands with respect to the UV maximum absorption.

4. Conclusions

On the basis of the obtained results the following concluding remarks can be drawn:

1. Novel optically active polymethacrylates based on the L-lactic acid residue and the azobenzene chromophore substituted in 4′-position by either cyano or nitro group have been synthesized and fully characterized. 2D NMR spectroscopy allowed the assignment of signals in the ^1H and ^{13}C NMR spectra of the investigated samples. An appreciable contribution of charge transfer mesomers to the electronic distribution of the photochromic chromophore was also demonstrated. Evaluation of ^{13}C T_1 relaxation times evidenced the rather limited mobility

of azobenzene chromophores when inserted in the macromolecules.

2. Irradiation at 360 nm induced a *trans* to *cis* isomerization of azobenzene moieties. Within the limits of experimental errors, the photoisomerization rate resulted independent of molecular weight, whereas an appreciable influence of the electron-withdrawing substituent of azobenzene chromophores was observed.
3. The large increase of optical activity of the polymers as compared with the corresponding low molecular weight models indicates that the former systems assume a higher conformational rigidity with a predominant chirality.
4. The chiroptical properties of the polymers, as revealed by CD measurements, seem to suggest that, on increasing the electron withdrawing character of the substituent on 4′-position of the azobenzene chromophore, a decrease of the conformational order of the macromolecules with a prevailing handedness occurs. This is also evidenced by the different dependence of the conformational arrangement of the macromolecules on changing the polarity of the solvent in polymers characterized by various electron withdrawing group on the azobenzene chromophore.

Acknowledgements

The financial support from C.N.R. and M.U.R.S.T. is gratefully acknowledged.

References

[1] Angiolini L, Caretti D, Carlini C, Salatelli E. Macromol Chem Phys 1995;196:2737.
[2] Angiolini L, Caretti D, Giorgini L, Salatelli E, Altomare A, Carlini C, Solaro R. Polymer 1998;39:6621.
[3] Angiolini L, Caretti D, Carlini C, Giorgini L, Salatelli E. Macromol Chem Phys 1999;200:390.
[4] Kim N. Macromol Symp 1996;101:235.
[5] Borsook H, Huffman HM, Liu YP. J Biol Chem 1933;102:449.
[6] Handbook of chemistry and physics, 62nd ed. Boca Raton:CRC Press, 1981. p. C-357.
[7] Moore JS, Stupp SI. Macromolecules 1990;23:65.
[8] Dutt S. J Chem Soc 1926:1171.
[9] Ringsdorf H, Schimdt HW. Makromol Chem 1984;185:1327.
[10] Brode WR. Ber 1928;61:1722.
[11] Brode WR, Seldin IL, Spoerri PE, Wyman GM. J Am Chem Soc 1955;77:2762.
[12] Angiolini L, Carlini C. J Polym Sci A: Polym Chem 1991;29:1455.
[13] Angiolini L, Caretti D, Carlini C. J Polym Sci A: Polym Chem 1994;32:1159.
[14] Silverstein RM, Bassler GC, Morrill TC. Spectrometric identification of organic compounds, 5. New York: Wiley, 1991.
[15] Altomare A, Ciardelli F, Ghiloni MS, Solaro R. Gazz Chim Ital 1997;127:143.
[16] Altomare A, Andruzzi L, Gallot B, Ciardelli F, Solaro R. Polym Int 1998;47:419.
[17] Wehrli CFW, Wirthlin T. Interpretation of carbon-13 NMR spectra, London: Heyden, 1978.
[18] Solaro R, Altomare A. Polymer 1990;31:1415.
[19] Altomare A, Lima R, Solaro R. Polymer 1991;2:3091.
[20] Randall JC. Polymer sequence determination. Carbon-13 NMR method, New York: Academic Press, 1977.
[21] Altomare A, Carlini C, Ciardelli F, Solaro R, Houben JL, Rosato N. Polymer 1983;24:95.
[22] Jaffe HH, Orchin M. Theory and application of ultraviolet spectroscopy. In: Jaffe HH, editor. New York: Wiley, 1962.
[23] Tinoco Jr I. J Am Chem Soc 1960;82:4785.
[24] Okamoto K, Itaya A, Kusabayashi S. Chem Lett 1974:1167.
[25] Chiellini E, Solaro R, Galli G, Ledwith A. Macromolecules 1980;13:1654.
[26] Majumdar RN, Carlini C. Makromol Chem 1980;181:201.
[27] Hiemstra H, Wynberg H. J Am Chem Soc 1981;103:417.